

Elimination of resonant divergences from QED in super-strong magnetic fields

Carlo Graziani*

*Laboratory for High-Energy Astrophysics, Code 665, NASA Goddard Space Flight Center,
Greenbelt, MD 20771*

Alice K. Harding

*Laboratory for High-Energy Astrophysics, Code 665, NASA Goddard Space Flight Center,
Greenbelt, MD 20771*

Ramin Sina

*University of Maryland Department of Physics, College Park, MD 20742
(November 15, 1994)*

Abstract

We study the resonant divergences that occur in quantum scattering cross-sections in the presence of a strong external magnetic field. We demonstrate that all such divergences may be eliminated by introducing radiative corrections to the leading-order scattering amplitudes. These corrections impose a choice of basis states that must be used in scattering calculations: electron states must diagonalize the mass operator, while photon states must diagonalize the polarization operator. The radiative corrections introduce natural line-widths into the energy denominators of all propagators, as well as into the time-development exponentials of all scattering states corresponding to external lines. Since initial and final scattering states may now decay, it is logically necessary to compute scattering amplitudes for a finite time-lapse between the preparation of the initial state and the measurement of the final state. Strict energy conservation, which appeared in previous formulations of the theory, must thus be abandoned. We exhibit the generic formulae for the scattering cross-sections in two useful limits, corresponding to the cases where either the initial states or the final states are stable, and discuss the application of the general formula when neither of these limits applies.

12.20.-m,11.10.st,97.60.Jd

Typeset using REVTeX

*E-Mail Address: carlo@twinkie.gsfc.nasa.gov

I. INTRODUCTION

Astrophysicists have had a long-standing interest in the physics of elementary processes in super-strong magnetic fields, with field strengths $B \gtrsim 10^{12}$ G. The cyclotron lines observed in the spectra of Her X-1 [1] and of 4U 0115+63 [2] as well as in many other X-ray pulsars have energy centers which correspond to field intensities in this range. There is also evidence for such field strengths in the spin-down rates of radio pulsars. If the spin-down is attributed to energy loss to electromagnetic radiation from a spinning magnetic dipole, many observations are consistent with field strengths of the order of 10^{12} - 10^{13} G, with some pulsar field strengths well in excess of even 10^{13} G [3,4]. In addition, there is tantalizing evidence for cyclotron lines in the spectra of gamma-ray bursts seen by the gamma-ray burst detector aboard the GINGA satellite [5], with line center energies consistent with field intensities of order 10^{12} G.

The association of Soft Gamma Repeaters with supernova remnants provides indirect evidence for even stronger fields. If the 8 s periodicity of the March 5 1979 event is identified with the rotation period of the neutron star, the known age of the N49 remnant may be used to estimate that the field strength is approximately 6×10^{14} G [6]. Moreover, such a strong field could help resolve the puzzle of how the March 5 1979 event could ostensibly have been so extravagantly in excess of the Eddington limit ($L \approx 10^4 L_{\text{Edd}}$), by suppressing the Thomson cross-section for photons propagating nearly parallel to the field lines [7].

In fields such as these, comparable in strength to the critical field strength $B_c \equiv m^2 c^3 / e \hbar = 4.414 \times 10^{13}$ G, all calculations of elementary processes must be carried out using Quantum Electrodynamics. There have been many such calculations over the past two decades, covering topics such as cyclotron absorption [8], cyclotron decay [9,10], single photon pair production [11,12], pair annihilation to a single photon [13–16], Compton scattering [17–20], two photon pair production [21], two photon pair annihilation [13,14], $e^- e^-$ scattering [22], and several more. All these processes have very different behavior from their $B = 0$ counterparts (if those counterparts are even possible), on account of the peculiar kinematics, as well as the discrete electronic states (Landau levels) associated with a uniform external magnetic field.

These calculations have always been carried out in the Furry picture, in close analogy to the $B = 0$ Feynman rules. The free space electron propagator is replaced by a propagator which is a Green's function for the Dirac equation in the external field, and the external fermion lines are represented by solutions of that equation. The results have often been interesting and useful, but they have not been uniformly satisfactory. The leading order calculation of resonant Compton scattering yields results which are divergent at the cyclotron resonances [17,18], evidently because to this order the theory makes no provision for natural line width. The line width may be included “by hand” in the results, making the cyclotron resonances finite [19,20]. However, there are other such “resonant divergences” in Compton scattering, which have nothing to do with the cyclotron resonances and which are not nearly as tractable [17,18]. In fact, one such resonance, which occurs exactly at the threshold where the initial photon may pair-produce, is responsible for making the total Compton cross-section divergent *everywhere* above this threshold.

In fact, the theory of elementary processes in external magnetic fields is plagued with such divergences. With a little practice, it is not hard to discover divergences resembling these *in every single process of second or higher order*. Clearly, this is a troublesome development

that casts a shadow upon the entire undertaking.

These resonant divergences occur because the kinematics of these processes allow intermediate “virtual states” to be real — that is, on-shell. Often, the on-shell intermediate state is an excited state, such as an electron in an excited Landau level, or a photon above the one photon pair-production threshold. In this case there is an associated decay width that may be pressed into service to control the divergence. The Weisskopf-Wigner broadening prescription,

$$E \rightarrow E - \frac{1}{2}i\Gamma, \tag{1.1}$$

when applied to the energy denominators in the propagator, pushes the poles in the propagator off the real axis, so that while the intermediate states may still be on-shell the propagator no longer diverges there. This is in fact the approach that has been adopted for Compton scattering [19,20,23], and which ascribes the natural line width to the cyclotron resonances.

However, there are circumstances in which a *stable* on-shell intermediate state may be produced. Such states are not attended by a decay width, so the associated divergence may not be reined in as before.

It should be pointed out that these divergences are entirely unrelated to the notorious ultraviolet divergences of QED. They are not the consequence of improper manipulation of field-theoretic distributions; rather, they occur whenever the circumstances of the elementary process permit a kinematically accessible on-shell intermediate state (KAOSIS). It is easy to recognize when a KAOSIS is permitted. For example, a second-order process will allow one if it may be viewed as a succession of two real first-order processes. Thus the KAOSIS corresponding to cyclotron resonance occurs because the process may be viewed as a real cyclotron absorption followed by a real cyclotron emission. Similarly, the second “disastrous” resonance in Compton scattering is due to a KAOSIS that corresponds to the initial photon undergoing a real decay to a pair, followed by the resulting positron annihilating with the initial electron to produce the final photon. The reason this KAOSIS is catastrophic is that the intermediate positron may be in the Landau ground state, so that no decay width is available to restrain the divergence.

At the same time, there is a second defect of the theory which so far has not received recognition as a problem. The calculation of S-matrix elements as outlined above always results in a δ -function which enforces strict energy conservation between initial and final states. This remains true even if some of these scattering states are unstable. But this is not physically sensible; the energy of an unstable state is only known to within its decay width, so that it is ludicrous to demand strict energy conservation for such transitions. Nevertheless, the current theory does so irrespective of whether or not the states are stable. As an example, the calculation of the decay of an electron in an excited Landau state produces the result that the emitted cyclotron photon is monochromatic, rather than having the Lorentzian line shape characteristic of resonant decay [9,10].

The difficulties of resonant divergence and of spurious energy conservation are related. Briefly, a stable KAOSIS may only occur if some of the particles in the initial and final states are themselves unstable, and it is their decay widths that restrain the divergence. However, the introduction of these decay widths smears out their energy, so that energy conservation (which was a consequence of their assumed eternal duration) no longer obtains.

Thus it appears that we must modify the current theory somehow if we are to circumvent these unphysical features. That modification is the purpose of this work. We demonstrate below that radiative corrections modify the propagators and the scattering states by introducing their respective decay widths into the S-matrix elements. In this sense, we are extending the results of Graziani [23], who carried out this program for the electron propagator only. The corrected “dressed” states and propagators result in scattering cross-sections that are always finite.

In Sec. II we discuss the role of the bare propagators in producing resonant divergences. In Sec. III we review the work of reference [23] on the electron propagator, which we extend to the photon propagator in Sec. IV. We exhibit the corrections to the scattering states in Sec. V. In Sec. VI we derive the modification of the S-matrix elements, and exhibit two useful limits: the absorption limit and the emission limit, wherein the initial and final states are stable, respectively. Finally, in Sec. VII we discuss the applicability of these results and the extent of the modification from the “standard” theory.

II. RESONANT DIVERGENCES AND PROPAGATORS

We begin with a discussion of the role that the bare electron and photon propagators have in producing the resonant divergences. In this section and throughout the rest of this work we use the metric signature $[+1, -1, -1, -1]$.

The bare electron propagator is simply expressed in terms of the fermion one-particle states. We work in the Furry picture, so these states are represented by solutions $\Psi_A^{(\eta)}$ of the Landau-Dirac (L-D) equation, that is, the Dirac equation in the presence of a classical, uniform, external magnetic field:

$$[\gamma^\mu(i\partial_\mu - eA_\mu) - m]\Psi_A^{(\eta)} = 0. \quad (2.1)$$

Here, $\eta = \pm 1$ refers to whether the solution has positive or negative energy, while A is the set of quantum numbers that specify the state — Landau level number, x^3 -momentum, spin, and an orbit center coordinate. We choose the gauge $A^0 = 0$, $\mathbf{A} = Bx^1\mathbf{e}_2$ for the external magnetic field, which is directed in the \mathbf{e}_3 direction. We also choose the orbit center coordinate a to be the x^1 Cartesian coordinate of the orbit center. With these choices, the functional dependence of the solutions of Eq. (2.1) is that of a plane wave in the x^2 and x^3 coordinates, while the x^1 dependence is that of a one-dimensional harmonic oscillator eigenfunction centered about $x^1 = a$ [25,26].

It is convenient to separate out the time dependence of $\Psi_A^{(\eta)}$:

$$\Psi_A^{(\eta)}(x) = e^{-i\eta E_A x^0} \phi_A^{(\eta)}(\mathbf{x}), \quad (2.2)$$

where $\phi_A^{(\eta)}(\mathbf{x})$ is an eigenstate of the Landau-Dirac Hamiltonian with quantum numbers A and eigenvalue E_A . E_A is given by $E_A = [m^2 + (p^3)^2 + 2mN\omega_B]^{1/2}$, where N is the Landau level number, p^3 is the momentum in the x^3 direction, and ω_B is the Larmor frequency. The bare electron propagator $G_B(x, y)$ may be represented in terms of the $\phi_A^{(\eta)}$:

$$G_B(x, y) = \sum_{A, \eta} \int \frac{dp^0}{2\pi} e^{-ip^0(x^0 - y^0)} \frac{\phi_A^{(\eta)}(\mathbf{x}) \overline{\phi_A^{(\eta)}}(\mathbf{y})}{p^0 - \eta(E_A - i0)}. \quad (2.3)$$

It is easy to verify that the expression in Eq. (2.3) is a Green's functions for Eq. (2.1) with the required boundary conditions [24]. We write $G_B(x, y)$ rather than $G_B(x - y)$ because neither Eq. (2.1) nor its Green's functions are translationally invariant — they are invariant under combinations of translations and gauge transformations.

The bare electron propagator enters the leading order calculation of such processes as Compton scattering, pair annihilation to two photons, and two photon pair production. The S-matrix elements for these processes are obtained by sandwiching $G_B(x, y)$ between appropriate fermion and photon states and integrating over x and y . These processes all exhibit resonant divergences. The proximate cause of those divergences is evidently the energy denominator in Eq. (2.3). The convolution of the propagator with the initial and final states fixes the values of p^0 and p^3 at the total energy and x^3 -momentum of the states, respectively. Thus, the residual energy-related degree of freedom in the summation over intermediate states is the Landau level number N , a non-negative integer. It follows that the energy denominator in Eq. (2.3) may be zero if the energy and x^3 -momentum of the scattering states are suitably tuned to one of the Landau levels. If this happens a resonant divergence occurs.

The bare photon propagator has the usual “transverse” expression

$$D_B(x - y)^{\mu\nu} = \int \frac{d^4k}{(2\pi)^4} (-g^{\mu\nu} + k^\mu k^\nu / k^2) \frac{e^{-ik(x-y)}}{k^2 + i0}. \quad (2.4)$$

It enters the calculation of S-matrix elements for processes such as electron-electron scattering [22] and electron-positron scattering. These processes have total cross-sections which exhibit resonant divergences. This may seem surprising at first, since the S-matrix elements for these processes are entirely finite, even when a KAOSIS is present. There is a key difference between the photon and electron propagators: In the electron case the on-shell energy contains a dependence on the Landau level quantum number, a discrete degree of freedom. Thus the resonances are “spaced-out” and well-separated. On the other hand, the photon on-shell energy is entirely dependent on the purely continuous degrees of freedom \mathbf{k} , and the “sum over intermediate states” is really an integral. While this integral will undoubtedly encounter any KAOSIS singularity, the small imaginary part in the denominator of the propagator provides a perfectly straightforward prescription for circumventing the pole. Thus the S-matrix elements are finite for these processes. Nevertheless, whenever an on-shell intermediate state is kinematically accessible, the total cross-sections diverge. What is going on?

The divergence is evident in the expressions in Appendix C of Langer [22] for the e-e scattering cross-section. Langer performed the integrals over the intermediate states simultaneously with those over final states and the average over initial states, in order to take advantage of several simplifications that ensue. Unfortunately, these manipulations obscure the source of the divergences. In order to shed some light on the situation, we have calculated cross-sections for e-e and e^+e^- scattering by computing the S-matrix elements before summing over final and averaging over initial states.

What we have found can be best illustrated by considering the specific example of e^+e^- scattering. As depicted in Fig. 1, there are two relevant Feynman diagrams. We have confirmed that in each case the S-matrix elements are finite even when there is a KAOSIS.

When a KAOSIS exists, however, there is a divergence resulting from the sum over *final* states. In the diagram of Fig. 1(a), the divergence arises from the integral over the variable $s = a_f^+ - a_f^-$, where a_f^+ and a_f^- are the orbit center x^1 -coordinates of the final positron and electron, respectively. In the diagram of Fig. 1(b), the divergence is due to the integral over the variable $t = a_f^- - a_i^-$, where a_i^- is the orbit center x^1 -coordinate of the initial electron.

We see, then, that the divergence manifests itself as an infinite range of interaction. When a KAOSIS is present, the intermediate photon may travel an arbitrarily large distance between its emission and its absorption without a reduction in amplitude. Consequently there is no spatial cutoff in the interaction, and the resulting integral over orbit center separation diverges.

The situation may be further clarified by explicitly computing the interaction range in the x^1 direction. When we calculate an S-matrix element for these processes, we integrate the bare photon propagator $D_B(x - y)^{\mu\nu}$ multiplied by two fermion currents, one for each vertex. Since our states are chosen to be plane waves in the x^2 - x^3 direction, the currents are also plane waves in x^2 and x^3 , and the integrals over x^0 , x^2 , and x^3 are tantamount to Fourier transforms of the photon propagator in those coordinates. The remaining integral over x^1 folds together two (in general well-separated) current functions $j_x(x^1)^\mu$, $j_y(y^1)^\nu$ with the transformed propagator $f_B(x^1 - y^1; k^0, k^2, k^3)g_{\mu\nu}$. We may easily compute $f_B(x^1; k^0, k^2, k^3)$. If we define $\rho \equiv (k^0)^2 - (k^2)^2 - (k^3)^2 = \pm q^2$, with $q \geq 0$, we find

$$f_B(x^1; k^0, k^2, k^3) = \begin{cases} -\frac{i}{2q}e^{iq|x^1|} & \text{if } \rho \geq 0, \\ -\frac{1}{2q}e^{-q|x^1|} & \text{otherwise.} \end{cases} \quad (2.5)$$

Thus, if $\rho \geq 0$ (the condition for the existence of a KAOSIS), the effective interaction range is infinite, whereas it is of finite range $\sim 1/q$ otherwise.

The situation is reminiscent of Coulomb scattering. If a wave packet scatters with large impact parameter from the center of the Coulomb potential, the momentum transfer is very low, and thus the exchanged photon is very close to its mass-shell (that is, its k vector is very near the apex of the light cone). This is the reason that the total Coulomb cross-section is divergent — the extreme infrared photons, which are nearly on-shell, give the interaction an infinite range. There is one noteworthy difference here, however: for the processes we consider, the virtual photons do not need to be infinitely soft to be on-shell, so that these resonant divergences are in no sense infra-red divergences.

As a consequence of this analysis, the cure for photon-propagator-related resonant divergences will necessarily have a slightly different mathematical character from that for the divergences that arise in connection with the electron propagator. While in the latter case we need to show how the previously diverging amplitudes may be made to converge, in the former case we must show how the previously long-range “effective interaction” may have its range curtailed.

III. THE DRESSED ELECTRON PROPAGATOR

The necessity of complexifying the energy denominator of the electron propagator so as to obtain the Weisskopf-Wigner line shape has been recognized for some time [19,20],

although these authors lacked a formal justification for their *ad hoc* complexification of the energy, given in Eq. (1.1). Graziani [23] provided this justification by considering radiative corrections to the electron propagator. As it turns out, the same procedure may be applied to the photon propagator as well. Quite generally, one finds that the operator which represents the self-interaction (the mass operator Σ in the case of the electron, the polarization operator Π in the case of the photon) singles out those solutions of the wave equation in which it is diagonal. The dressed propagator may then be expressed as a sum over all such states, with the energy in the denominator acquiring an imaginary part given by Eq. (1.1). We review the discussion of the electron propagator from Ref. [23], and extend it to the photon propagator in the next section.

The dressed propagator $G(x, y)$ is related to the bare propagator and the self-energy operator $\Sigma(x, y)$ by the Dyson equation $G = G_B + G_B \cdot \Sigma \cdot G$, where the dot denotes four-dimensional convolution as well as spinorial matrix multiplication. It follows that $G(x, y)$ is a Green's function for the dressed L-D operator

$$[\gamma^\mu(i\partial_\mu - eA_\mu) - m - \Sigma] \cdot \Psi_A^{(\eta)} = 0. \quad (3.1)$$

Now, let $\Theta_{p^0 A}^{(\eta)}(x) = e^{-ip^0 x^0} \phi_A^{(\eta)}(\mathbf{x})$. It may be shown [26,27,23] that Θ diagonalizes Σ if the $\phi_A^{(\eta)}$ are simultaneous eigenstates of the Landau-Dirac Hamiltonian and of the x^3 -component of the magnetic moment operator of Sokolov and Ternov [28]. This condition defines what is meant by “spin up” and “spin down”, in the absence of the tools provided by Poincaré group representation theory (the physical system no longer has full Poincaré invariance). If this condition is satisfied, *and only in this case*, G may be represented in a form analogous to Eq. (2.3):

$$G(x, y) = \sum_{A, \eta} \int \frac{dp^0}{2\pi} e^{-ip^0(x^0 - y^0)} \frac{\phi_A^{(\eta)}(\mathbf{x}) \overline{\phi_A^{(\eta)}}(\mathbf{y})}{p^0 - \eta(E_A - i0) - \Sigma(p^0, A, \eta)}, \quad (3.2)$$

where $\Sigma(p^0, A, \eta)$ is the diagonal matrix element of Σ in the state $\Theta_{p^0 A}^{(\eta)}$. It is in general a complex number, in contradistinction to the case where the external field strength is zero, where the diagonal matrix elements of the self-energy operator are real. The real part of $\Sigma(p^0, A, \eta)$ merely yields a small shift in the energy of the state, while the imaginary part provides a line-width to the otherwise divergent resonant energy denominator. This justifies neglecting the real shift while preserving the imaginary width. It was shown explicitly in Ref. [23] that in this approximation, the pole in the propagator corresponding to state A , η is located at $p^0 = \eta(E_A - \frac{i}{2}\Gamma_A)$, where Γ_A is just the Weisskopf-Wigner decay rate of the state A , computed to leading order:

$$\Gamma_A = e^2 \int \frac{d^3\mathbf{k}}{2\omega_k(2\pi)^3} \sum_{\epsilon} \sum_B |T_{AB}(\mathbf{k}, \epsilon)|^2 (2\pi) \delta(E_A - E_B - \omega_k). \quad (3.3)$$

Here, $T_{AB}(\mathbf{k}, \epsilon)$ is the interaction matrix element for the transition from the state A to the state B with the emission of a photon with wave vector \mathbf{k} and polarization ϵ . It follows that the dressed propagator may be expressed as

$$G(x, y) = \sum_{A, \eta} \int \frac{dp^0}{2\pi} e^{-ip^0(x^0 - y^0)} \frac{\phi_A^{(\eta)}(\mathbf{x}) \overline{\phi_A^{(\eta)}}(\mathbf{y})}{p^0 - \eta(E_A - i\Gamma_A/2)} \quad (3.4)$$

$$= -i \sum_{A, \eta} \eta \theta[\eta(x^0 - y^0)] e^{-i\eta(E_A - i\Gamma_A/2)(x^0 - y^0)} \phi_A^{(\eta)}(\mathbf{x}) \overline{\phi_A^{(\eta)}}(\mathbf{y}) \quad (3.5)$$

to first order in e^2 .

It appears from these equations that the prescription of Eq. (1.1) is in fact rigorously justifiable. We wish to emphasize, however, that Eqs. (3.4)-(3.5) are only correct when the states $\phi_A^{(\eta)}$ are chosen so that the $\Theta_{p^0 A}^{(\eta)}$ diagonalize the self-energy operator, or equivalently, so that the $\phi_A^{(\eta)}$ diagonalize the x^3 -component of the Sokolov-Ternov magnetic moment operator. The states of Sokolov and Ternov [28], and those of Herold, Ruder, and Wunner [10] satisfy these conditions, and their use leads to correct expressions for the scattering cross-sections. The states of Johnson and Lippmann [25], which have gained some currency in the literature, do not satisfy the required conditions [26]. In particular, as discussed in [23], the use of Johnson-Lippmann states in the computation of cyclotron scattering cross-sections can lead to relative errors of order 45% at the first cyclotron harmonic, depending on the field strength.

IV. THE DRESSED PHOTON PROPAGATOR

The procedure for the photon propagator is entirely analogous to the one followed for the electron propagator. The self-interaction of the Maxwell field is represented by the polarization operator $\Pi(x - y)^{\mu\nu}$, which satisfies the condition of gauge invariance, $\frac{\partial}{\partial x^\mu} \Pi(x - y)^{\mu\nu} = 0$. The dressed photon propagator $D(x - y)^{\mu\nu}$ is obtained from the bare propagator $D_B(x - y)^{\mu\nu}$ and $\Pi(x - y)^{\mu\nu}$ by solving the Dyson equation $D = D_B + D_B \cdot \Pi \cdot D$. In order to accomplish this, it is necessary to find the polarization states which diagonalize $\Pi^{\mu\nu}$, which are analogous to the spinor states that diagonalize Σ . These polarization states were found by Batalin and Shabad [29], and written explicitly for the case of a uniform magnetic field by Shabad [30]. For a photon with 4-momentum k propagating in a uniform magnetic field $\mathbf{B} = B\mathbf{e}_3$ we have the following three (unnormalized) polarization vectors:

$$b_{\perp}^{\mu} = k^2(e_1)^{\mu} - k^1(e_2)^{\mu}, \quad (4.1a)$$

$$b_{\parallel}^{\mu} = k^3(e_0)^{\mu} + k^0(e_3)^{\mu}, \quad (4.1b)$$

$$b_{\perp}^{\mu} = (k^{\nu} k_{\nu}) k_{\perp}^{\mu} - (k_{\perp}^{\nu} k_{\perp\nu}) k^{\mu}, \quad (4.1c)$$

where $k_{\perp}^{\mu} = k^1(e_1)^{\mu} + k^2(e_2)^{\mu}$, and $(e_{\rho})^{\mu}$ is a unit vector in the x^{ρ} direction. These modes diagonalize the Fourier-transformed polarization operator $\Pi(k)^{\mu\nu} = \int d^4x \Pi(x)^{\mu\nu} e^{ikx}$. There are three of them, because by gauge invariance Π satisfies $k_{\mu} \Pi(k)^{\mu\nu} = 0$, so that the fourth mode is just k , and the eigenvalue of Π that corresponds to it is zero. The mode b_{\parallel} is so labeled because on shell it differs from the usual ‘‘parallel’’ polarization 3-vector by an

inessential multiple of k , while b_\perp is just the usual ‘‘perpendicular’’ mode. The vector b_L represents a longitudinal mode, which on shell is proportional to k . The b in Eqs. (4.1) are orthogonal to each other, and to k .

Using these modes, the transverse photon propagator may be expressed as follows:

$$D(x-y)^{\mu\nu} = - \int \frac{d^4k}{(2\pi)^4} e^{-ik(x-y)} \sum_j \frac{b_j^\mu b_j^\nu}{b_j \cdot b_j} \frac{1}{(k^0)^2 - \omega_k^2 + \Pi(k^0, \mathbf{k}, j)}, \quad (4.2)$$

where

$$\Pi(k^0, \mathbf{k}, j) \equiv \Pi(k)_{\mu\nu} b_j^\mu b_j^\nu / (b_j \cdot b_j). \quad (4.3)$$

To first order in e^2 , the pole in Eq. (4.2) is located at $(k^0)^2 = \omega_k^2 - \Pi(\omega_k, \mathbf{k}, j)$, so that to this order Eq. (4.2) may be written

$$D(x-y)^{\mu\nu} = - \int \frac{d^4k}{(2\pi)^4} e^{-ik(x-y)} \sum_j \frac{b_j^\mu b_j^\nu}{b_j \cdot b_j} \frac{1}{(k^0)^2 - \omega_k^2 + \Pi(\omega_k, \mathbf{k}, j)}. \quad (4.4)$$

Note that when the light-cone condition $k^0 = \omega_k$ is satisfied, both b_\perp and b_\parallel are space-like ($b \cdot b < 0$) while the longitudinal mode b_L is light-like. It follows that $\Pi(\omega_k, \mathbf{k}, L) = 0$, so we only need compute $\Pi(\omega_k, \mathbf{k}, j)$ for $j = \perp, \parallel$.

The (unrenormalized) leading-order expression for $\Pi(x-y)^{\mu\nu}$ is

$$\Pi(x-y)^{\mu\nu} = -ie^2 \text{Tr}(G_B(y, x) \gamma^\mu G_B(x, y) \gamma^\nu). \quad (4.5)$$

Following the analogy to the case of the electron propagator, we calculate the imaginary part of the diagonal matrix elements of $\Pi^{\mu\nu}$, while neglecting the real part. For this purpose, Eq. (4.5) is entirely adequate, even though it is not renormalized. The renormalization counter-terms which are to be subtracted from the diagonal matrix elements of $\Pi^{\mu\nu}$ are purely real, so that the imaginary parts are unaffected by renormalization.

This expression for $\Pi^{\mu\nu}$ is in fact translationally invariant, even though G_B is not. The translational invariance may be established using the ‘‘translation+gauge transformation’’ invariance of G_B alluded to in the previous subsection [31].

Substituting Eq. (2.3) into Eq. (4.5), after some manipulation we obtain

$$\Pi(x-y)^{\mu\nu} = -e^2 \sum_{A, A', \eta} \int \frac{dp^0}{2\pi} e^{-ip^0(x^0-y^0)} \frac{\overline{[\phi_A^{(\eta)}(\mathbf{x}) \gamma^\mu \phi_{A'}^{(-\eta)}(\mathbf{x})]} [\phi_{A'}^{(-\eta)}(\mathbf{y}) \gamma^\nu \phi_A^{(\eta)}(\mathbf{y})]}{\eta p^0 + E_A + E_{A'} - i0}. \quad (4.6)$$

We now Fourier transform this equation. Taking the implicit translation invariance into account, we obtain

$$\begin{aligned} \Pi(k)^{\mu\nu} \epsilon_\mu \epsilon_\nu &= L^{-3} T^{-1} \int d^4x d^4y e^{ik(x-y)} \Pi(x-y)^{\mu\nu} \epsilon_\mu \epsilon_\nu \\ &= -2\omega_k \sum_{A, A', \eta} \frac{|J_{AA'}^{(\eta)}(\mathbf{k})^\mu \epsilon_\mu|^2}{\eta k^0 + E_A + E_{A'} - i0}, \end{aligned} \quad (4.7)$$

where

$$J_{AA'}^{(\eta)}(\mathbf{k})^\mu \equiv e^2 L^{-3/2} (2\omega_k)^{-1/2} \int d^3\mathbf{x} \overline{\phi_A^{(\eta)}}(\mathbf{x}) \gamma^\mu \phi_{A'}^{(-\eta)}(\mathbf{x}) e^{i\mathbf{k}\cdot\mathbf{x}}. \quad (4.8)$$

When ϵ^μ is a normalized polarization vector, $J_{AA'}^{(+)}(\mathbf{k})^\mu \epsilon_\mu$ is just the interaction matrix element for a transition from a photon with wave vector \mathbf{k} and polarization ϵ to a pair with quantum numbers $A'A$. The imaginary part of Eq. (4.7) is

$$\text{Im}[\Pi(k)^{\mu\nu} \epsilon_\mu \epsilon_\nu] = -2\omega_k \sum_{A,A'} \left| J_{AA'}^{(+)}(\mathbf{k})^\mu \epsilon_\mu \right|^2 \pi \delta(E_A + E_{A'} - |k^0|), \quad (4.9)$$

where we have used the identity $\sum_{AA'} \left| J_{AA'}^{(+)}(\mathbf{k})^\mu \epsilon_\mu \right|^2 = \sum_{AA'} \left| J_{AA'}^{(-)}(\mathbf{k})^\mu \epsilon_\mu \right|^2$, a consequence of the parity invariance of Eq. (2.1).

Comparing with Eq. (4.3), we see that to obtain the imaginary part of $\Pi(\omega_k, \mathbf{k}, j)$, we may impose the light-cone condition $k^0 = \omega_k$ and let $\epsilon_\mu = (\epsilon_j)_\mu = (b_j)_\mu / |b_j \cdot b_j|^{1/2} \Big|_{k^0=\omega_k}$ in Eq. (4.9), keeping in mind that $b_j \cdot b_j < 0$. The result is

$$\begin{aligned} \text{Im}[\Pi(\omega_k, \mathbf{k}, j)] &= 2\omega_k \sum_{A,A'} \left| J_{AA'}^{(+)}(\mathbf{k})^\mu (\epsilon_j)_\mu \right|^2 \pi \delta(E_A + E_{A'} - \omega_k) \\ &= 2\omega_k \times \Gamma(\mathbf{k}, j)/2. \end{aligned} \quad (4.10)$$

Clearly, $\Gamma(\mathbf{k}, j)$ is just the Weisskopf-Wigner decay rate of the photon state (\mathbf{k}, j) . The energy denominator in Eq. (4.4) is thus $(k^0)^2 - \omega_k^2 + 2i\omega_k \Gamma(\mathbf{k}, j)/2 \approx (k^0)^2 - (\omega_k - i\Gamma(\mathbf{k}, j)/2)^2$, to first order in e^2 . Consequently, the dressed photon propagator is

$$D(x-y)^{\mu\nu} = - \int \frac{d^4 k}{(2\pi)^4} e^{-ik(x-y)} \sum_j \frac{b_j^\mu b_j^\nu}{b_j \cdot b_j} \frac{1}{(k^0)^2 - (\omega_k - i\Gamma(\mathbf{k}, j)/2)^2}. \quad (4.11)$$

$$\begin{aligned} &= i \int \frac{d^3 \mathbf{k}}{(2\pi)^3 2\omega_k} \\ &\quad \times \sum_j \sum_{\eta=\pm 1} \frac{b_j^\mu b_j^\nu}{b_j \cdot b_j} \theta[\eta(x^0 - y^0)] e^{-i\eta(\omega_k - i\Gamma(\mathbf{k}, j)/2)(x^0 - y^0)} e^{i\eta \mathbf{k} \cdot (\mathbf{x} - \mathbf{y})}. \end{aligned} \quad (4.12)$$

We see that the prescription of Eq. (1.1) continues to hold in the case of the photon field. It should be emphasized, however, that it is essential that the polarization modes given in Eqs. (4.1) be used in the expression for the propagator in order for that expression to be correct.

Recalling the discussion at the end of Sec. II, we investigate the range of the ‘‘dressed’’ interaction by computing the partial Fourier transform of the propagator in Eq. (4.11) with respect to x^0 , x^2 , and x^3 . Assuming the presence of a KAOSIS (so that $q^2 = (k^0)^2 - (k^2)^2 - (k^3)^2 \geq 0$), we find for the transformed propagator $f(x^1; k^0, k^2, k^3)$,

$$\begin{aligned} f(x^1; k^0, k^2, k^3) &= -\frac{i}{2Z(q)} e^{iZ(q)|x^1|}, \\ Z(q) &\equiv \frac{1}{\sqrt{2}} \left(\sqrt{u^2 + q^2} + i\sqrt{u^2 - q^2} \right), \\ u^2 &\equiv \sqrt{q^4 + (k^0)^2 \Gamma(\mathbf{k}, j)^2}, \end{aligned} \quad (4.13)$$

where $\Gamma(\mathbf{k}, j)$ is evaluated at the point $k^1 = q$. Since the imaginary part of $Z(q)$ is positive, we find that the presence of a non-zero decay rate $\Gamma(\mathbf{k}, j)$ has cut off the interaction range.

Note that $Z(q) \rightarrow q$ as $\Gamma \rightarrow 0$, so that if the KAOSIS is below the one photon pair-production threshold the interaction range is not cut off (in fact we then have $f = f_B$, as expected). In the next section, we will show how the interaction range is cut off when the KAOSIS is below threshold. In the mean time though, we have already disposed of the resonant divergence associated with the process of Fig. 1(b), which always has a KAOSIS above the one photon pair-production threshold. Indeed, we may now give a useful interpretation of that divergence: it arose because the intermediate photon (which at the KAOSIS may be viewed as being due to a pair annihilation) was not instructed to decay to a pair in a finite time, so that it produced finite amplitude for the final pair at all values of x^1 . The resulting total cross-section was infinite. Now that the dressed propagator is used to calculate the S-matrix element, the photon is aware of its decay obligations, and the cross-section due to this process is finite.

V. CORRECTIONS TO SCATTERING STATES

The propagator corrections described in the previous section are sufficient to control resonant divergences in many processes and regimes. Nevertheless, there are still cases where a scattering process may lead to a divergent resonance. Specifically, any process exhibiting a KAOSIS with vanishing decay rate will exhibit divergent scattering cross-sections even if calculated using the dressed propagators.

Such processes are not at all rare. Consider the case of an electron scattering with a photon which is above the one photon pair-production threshold. The following two first-order processes correspond to an on-shell second-order process: first the photon pair-produces, then the initial electron annihilates with the newly produced positron to produce the final photon [see Fig. 2(a)]. If the intermediate on-shell positron is in the Landau ground state, its decay rate is zero, so that there is no line width supplied by the propagator to control the resulting divergence. This divergence represents something of a calamity, since its effect is to make the total cross-section for Compton scattering divergent everywhere above the one photon pair-production threshold [17,18].

A second example is provided by electron-electron scattering, in which at least one of the initial electrons is in an excited Landau state [Fig. 2(b)]. Once again, there is a second-order on-shell process that is analogous to a succession of two first order processes, in which the excited electron emits a cyclotron photon which is in turn absorbed by the other electron. If the on-shell photon is below the one photon pair-production threshold, its decay rate is zero, and there is a resonant divergence — see the expressions in Appendix C of Ref. [22].

It turns out that in every second-order process with a stable KAOSIS there are non-zero decay rates associated with the initial and final scattering states. Thus, in the first of the two examples above, the initial and final photons are capable of decay, while in the second example, there are excited Landau levels in both the initial and final states. One might hope, then, that the decay rates of the scattering states might be pressed into service to control the resonant divergences when the decay rate of the intermediate state is zero. As we now demonstrate, this is not only possible, it is a necessary feature of the same program

of radiative corrections that brought the decay rates into the propagators. That program demands that we should apply radiative corrections to the external lines, in addition to the propagators.

It might be objected at this point that loop corrections to external lines can have no bearing on the problem, since the arbitrary constants which arise during renormalization are in part fixed by the requirement that the external lines should suffer no corrections, so that the scattering states should continue to be represented by solutions of the “free” wave equation with the physical mass [32].

The answer to this objection is that in the present case, the limited number of arbitrary constants is not sufficient to satisfy the physical requirement above for all scattering states. For example, in the case of the electron field, we may *only* demand that the Landau ground state A_G propagate according to Eq. (2.1). Once we have used up the relevant renormalization constants to ensure this condition, the remaining excited Landau states must propagate according to Eq. (3.1). In other words, in Eq. (3.1) we may set $\Sigma(p^0 = \eta E_G, A_G, \eta) = 0$ (where E_G is the energy of the ground state), but then the remaining $A \neq A_G$ will yield non-zero on-shell, diagonal matrix elements of Σ . Similarly for the Maxwell field, we may only demand that $\Pi(\omega_k, \mathbf{k}, j) = 0$ in the limit $\mathbf{k} \rightarrow 0$, so that only infinitely soft photons see no refraction in the magnetized vacuum.

The origin of this “feature” of magnetic QED is the fact that excited scattering states are technically not scattering states at all, insofar as they do not correspond to asymptotic one-particle states of the quantum field which are stable. In principle, we should only use stable states as initial and final scattering states — electrons and positrons in the Landau ground state and photons below the one photon pair-production threshold. The consequence of this restriction on the theory would be that multiple scattering events and scatterings followed by multiple emissions could only be treated by computing scattering amplitudes corresponding to very high order Feynman diagrams, a notoriously burdensome task. Thus, some of the most interesting astrophysical applications of the theory would become virtually inaccessible.

As an alternative, we may represent such high-order multiple events as a succession of lower order transitions between states that are not necessarily stable, and treating those states as if they were genuine scattering states. For example, a process in which an electron in the ground state and a photon of energy above the third cyclotron harmonic make a resonant transition to a state with an electron in the ground state and four photons may be approximated by a Compton scattering event in which the final electron is left at the third harmonic, followed by three resonant decays.

This approximation of scattering states by excited states is a common one in the literature [18–21], but to date there has been no investigation of its validity and limitations, or of what modifications the usual Feynman perturbation theory must suffer in order to accommodate them. That investigation is the central concern of this work.

We now discuss the specific modifications to the scattering states due to radiative corrections. Consider a bare external electron line in a Feynman diagram which is represented in the scattering amplitude by the spinor $\Psi_A^{(\eta)}(x)$, a solution of Eq. (2.1). After subjecting the line to corrections associated with the self-energy operator Σ , the result is a dressed line represented by the spinor $\Theta_A^{(\eta)}(x)$, where

$$\begin{aligned}
\Theta_A^{(\eta)} &= \Psi_A^{(\eta)} + G_B \cdot \Sigma \cdot \Psi_A^{(\eta)} + G_B \cdot \Sigma \cdot G_B \cdot \Sigma \cdot \Psi_A^{(\eta)} + \dots \\
&= \Psi_A^{(\eta)} + G_B \cdot \Sigma \cdot \Theta_A^{(\eta)}.
\end{aligned} \tag{5.1}$$

If we view the L-D operator [the wave operator in Eq. (2.1)] as a “free Hamiltonian” and Σ as a perturbation, Eq. (5.1) may be cast as a four-dimensional Lippmann-Schwinger equation connecting an eigenstate $\Psi_A^{(\eta)}$ of the L-D operator with eigenvalue zero, to an eigenstate $\Theta_A^{(\eta)}$ of the dressed L-D operator [the wave operator in Eq. (3.1)], also with eigenvalue zero. In other words, $\Theta_A^{(\eta)}$ satisfies

$$[\gamma^\mu (i\partial_\mu - eA_\mu) - m - \Sigma] \cdot \Theta_A^{(\eta)} = 0. \tag{5.2}$$

It is a simple matter to find solutions of this equation, since we already know of states that simultaneously diagonalize the “free” operator and its perturbation. Substituting $\Theta_A^{(\eta)}(x) = e^{-ip^0 x^0} \phi_A^{(\eta)}(\mathbf{x})$ in Eq. (5.2), we find

$$p^0 = \eta(E_A - i\Gamma_A/2), \tag{5.3}$$

so that the dressed scattering state is

$$\Theta_A^{(\eta)}(x) = e^{-i\eta(E_A - i\Gamma_A/2)x^0} \phi_A^{(\eta)}(\mathbf{x}). \tag{5.4}$$

We may repeat the above argument for a bare external line which is represented by the Dirac conjugate spinor $\overline{\Psi}_A^{(\eta)}(x)$. The result is that the dressed state is $\overline{\Lambda}_A^{(\eta)}(x)$, where

$$\overline{\Lambda}_A^{(\eta)}(x) = e^{+i\eta(E_A - i\Gamma_A/2)x^0} \overline{\phi}_A^{(\eta)}(\mathbf{x}). \tag{5.5}$$

Note that $\overline{\Lambda}_A^{(\eta)}(x)$ is *not* the Dirac conjugate spinor of $\Theta_A^{(\eta)}(x)$, since the real part of the exponent changes sign.

The procedure is analogous for the external photon lines. The dressed states $a(x)^\nu$ are solutions of

$$(g_{\mu\nu}\square - \Pi_{\mu\nu})a^\nu = 0. \tag{5.6}$$

Using the polarization states of the previous section (for $j = \perp, \parallel$) to write

$$a_{\mathbf{k}j}(x)^\nu = (2\omega_k L^3)^{-1/2} (\epsilon_j)^\nu e^{-ik^0 x^0 + i\mathbf{k}\cdot\mathbf{x}}, \tag{5.7}$$

and substituting in Eq. (5.6), we obtain

$$k^0 = \pm[\omega_k - i\Gamma(\mathbf{k}, j)/2], \tag{5.8}$$

so that the dressed scattering state is

$$a_{\mathbf{k}j}(x)^\nu = (2\omega_k L^3)^{-1/2} (\epsilon_j)^\nu e^{\pm i[\omega_k - i\Gamma(\mathbf{k}, j)/2]x^0 - i\mathbf{k}\cdot\mathbf{x}}. \tag{5.9}$$

From Eqs. (5.4), (5.5), and (5.9) it is apparent that the prescription of Eq. (1.1) applies equally well to scattering states as to propagators. It is a general feature of this prescription

that the resulting positive and negative energy states are not conjugate to each other, since the real part of the exponent changes sign. Consequently, positive energy solutions decay as time increases, while negative energy solutions grow. This is in keeping with the interpretation of the negative energy solutions as particles which move backwards in time. In the application of these formulae to the calculation of S-matrix elements, the $e^{-i(E-i\Gamma/2)x^0}$ dependence is ascribed to initial states, while the $e^{+i(E-i\Gamma/2)x^0}$ dependence is ascribed to final states.

There is a second way of understanding the introduction of decay rates in the time-development exponentials of scattering states. We may take the view, discussed above, that the metastable scattering states are really approximations standing in for internal lines of much larger Feynman diagrams. That being the case, their functional form may be read directly from the components of their respective propagators, written in the forms of Eqs. (3.5) and (4.12).

The appearance of the decay rates in the time-development exponentials of the states will ultimately lead to their appearance in energy denominators of scattering amplitudes, after integration over time variables. Here, however, there appears a major difference with the usual practice of obtaining amplitudes. The real parts of the exponentials will lead in general to divergent expressions if the time integration limits are allowed to go to $\pm\infty$ as usual. It is not difficult to see physically why we should expect trouble in this limit. Letting the upper time limit go to infinity in the S-matrix element is tantamount to asking the question, “what is the probability of observing this decaying state in the infinitely distant future?” Clearly, no calculation is required to see that the answer must be “zero.” Similarly, letting the lower time limit go to minus infinity amounts to inquiring about an interaction at a finite time of a decaying state which was prepared in the infinitely distant past — a process which also has vanishing probability of occurrence.

It is therefore necessary that the scattering theory be formulated for states prepared at finite times T_i and measured at finite times T_f . Only when the initial state is stable may the limit $T_i \rightarrow -\infty$ be taken, and only when the final, measured state is stable may we set $T_f \rightarrow \infty$. These limits are termed the “absorption” and “emission” limits, for reasons that will shortly be made clear.

Note that due to the real parts in the time-development exponentials, the scattering states are not generally normalized to unit probability. In fact, they may only be so normalized at a given, fixed time. Physically, it is necessary to ensure that the initial states be normalized at the preparation time T_i , and that the final states be normalized at the measurement time T_f . This could be accomplished by setting $x^0 \rightarrow x^0 - T_i$ or $x^0 \rightarrow x^0 - T_f$, as appropriate, in the expressions of Eqs. (5.4), (5.5), and (5.9). It is often simpler to calculate the amplitudes with the states as written above and multiply the result by the factor $\exp[\frac{1}{2}(\Gamma_i T_i - \Gamma_f T_f)]$, where $\Gamma_{i(f)}$ is the sum of the decay rates of the particles in the initial (final) state.

There is an extremely important consequence of this finite-time formulation of the theory: *strict energy conservation no longer holds*. The energy conserving δ -functions which appeared in the old amplitudes were a consequence of the integration of time exponentials over all time. By the time-energy uncertainty relation, we may not determine the energy to infinite precision over a finite time interval. This is not an alarming consequence of the theory, but rather a desirable one. When we discuss the excitation or decay of metastable

states, we cannot expect to determine the energy of those states to better than the natural line width, so energy-conserving δ -functions should actually violate our physical intuition for these processes. In fact, we will see that strict energy conservation is recovered *only* when $\Gamma_i = \Gamma_f = 0$. Thus, for example, in the expressions of Herold [17] for Compton scattering from ground state to ground state, the energy-conserving δ -functions are appropriate.

We now discuss an example which provides a simple application of these ideas: cyclotron decay. Consider an electron which is prepared in an excited state A at a time $T_i = 0$. We calculate, to first order, the probability that the system should make a transition to the ground state A_G with the emission of a photon in the state (\mathbf{k}, j) , which is below the one photon pair-production threshold. Since $\Gamma_f = 0$, we may take the limit $T_f \rightarrow \infty$. The S-matrix element is given by

$$\begin{aligned} S_{fi} &= T_{A_G A}(\mathbf{k})_\mu (\epsilon_j)^\mu \int_0^\infty dx^0 e^{-i[(E_A - i\Gamma_A/2) - E_G - \omega_k]x^0} \\ &= \frac{-iT_{A_G A}(\mathbf{k})_\mu (\epsilon_j)^\mu}{E_A - E_G - \omega_k - i\Gamma_A/2}, \end{aligned} \quad (5.10)$$

where $T_{A_G A}(\mathbf{k})_\mu$ is the interaction matrix element for the transition:

$$T_{A_G A}(\mathbf{k})^\mu = e^2 L^{-3/2} (2\omega_k)^{-1/2} \int d^3\mathbf{x} e^{-i\mathbf{k}\cdot\mathbf{x}} \overline{\phi_{A_G}^{(+)}(\mathbf{x})} \gamma^\mu \phi_A^{(+)}(\mathbf{x}). \quad (5.11)$$

Note that in Eq. (5.10), the energy conserving δ -function has been replaced by the Wigner-Weisskopf line shape function. Thus, the new formalism has reproduced the well-known result from non-relativistic quantum mechanics, which the old formalism could not (compare Refs. [9–12,33]).

We close this section with a discussion of the effect of using the dressed electron scattering states of Eqs. (5.4) and (5.5) on the range of the interaction in the presence of a KAOSIS of the photon propagator below the one photon pair-production threshold. We may attempt to repeat the procedure that led to Eqs. (2.5) and (4.13). However, this time the computation of the S-matrix element corresponding to Fig. 1(a) is no longer equivalent to taking the Fourier transform of the photon propagator with respect to x^0 , since the dependence of the scattering states on x^0 is no longer purely oscillatory. Rather, the effective one-dimensional interaction $g(x^1; k^2, k^3)$ that results is given by

$$g(x^1; k^2, k^3) = \int \frac{dk^0}{2\pi} f_B(x^1; k^0, k^2, k^3) W(k^0 - E), \quad (5.12)$$

where $W(z)$ is a function which is only appreciable in a range $\pm\Delta$ about $z = 0$. The restricted domain of W is a reflection of the restricted domain in time of the scattering states — in fact, we have either $\Delta \sim \Gamma$ or $\Delta \sim (T_f - T_i)^{-1}$, whichever is largest.

By using stationary phase arguments, it is easy to see that $g(x^1; k^2, k^3)$ can only be appreciable for a limited range of $|x^1|$:

$$|x^1| \lesssim \frac{2\pi}{[(E + \Delta)^2 - (k^2)^2 - (k^3)^2]^{1/2} - [E^2 - (k^2)^2 - (k^3)^2]^{1/2}}. \quad (5.13)$$

Thus the range of the interaction is curtailed when the scattering states may decay. We see that the spurious infinite interaction range that entered calculations which used bare excited scattering states was a consequence of their assumed infinite duration. Once their limited duration is incorporated into the formalism, their interaction becomes short-ranged.

Note that a KAOSIS of the photon propagator may exist only if either some of the scattering states are excited or the KAOSIS itself is above the one photon pair-production threshold. Therefore, the scattering cross-sections for processes with virtual photons *are now always finite* if the dressed states and propagators are used to calculate them. We will show in the next section that resonant divergences are now also under control in processes with virtual fermions.

VI. SCATTERING FORMULAE

We now compute generic second-order formulae for two-particle to two-particle scattering. The Feynman diagram in Fig. 3 depicts such a process irrespective of whether the various lines represent fermions or photons. Our notation, which is illustrated in Fig. 3, is as follows. Let the energies of the external lines be E_ρ , and let their decay rates be Γ_ρ ($\rho = a, b, c, d$). Define $\mu_\rho = \pm 1$, with $\mu_\rho = +1$ if the line represents an incoming state and $\mu_\rho = -1$ if it represents an outgoing state. Let the lines with $\rho = a, b$ join at the vertex with coordinates x , and those with $\rho = c, d$ join at the vertex with coordinates y (see Fig. 3). Define $E_x \equiv \mu_a E_a + \mu_b E_b$, $\Gamma_x \equiv \mu_a \Gamma_a + \mu_b \Gamma_b$, and similarly for E_y and Γ_y . Also define the complex energies $\mathcal{E}_x \equiv E_x - \frac{i}{2}\Gamma_x$, $\mathcal{E}_y \equiv E_y - \frac{i}{2}\Gamma_y$.

Let the energies of the two initial particles be e_{i1} , e_{i2} , and let their decay rates be γ_{i1} , γ_{i2} . Also let the energies of the two final particles be e_{f1} , e_{f2} , and let their decay rates be γ_{f1} , γ_{f2} . The e and γ are set equal to the E and Γ as appropriate to the process under consideration, an identification illustrated by the passage from Fig. 3 to Fig. 4.

We denote the quantum state of the intermediate particle by l : $l = A$ if the particle is a fermion, $l = (\mathbf{k}, j)$ if it is a photon. The energy and decay rate of the intermediate state are E_l and Γ_l , respectively, and we define $\mathcal{E}_l \equiv E_l - \frac{i}{2}\Gamma_l$. We also introduce the index $\eta = \pm 1$, where $\eta = +1$ if the intermediate state has positive energy and $\eta = -1$ otherwise.

The propagators are given by Eqs. (3.5) and (4.12). The S-matrix element for the process is obtained by sandwiching the appropriate propagator between the scattering states in the usual way [32] and integrating over the space time coordinates x and y . The general result is

$$S_{fi} = i \sum_{l\eta} c_\eta M_{fi}(l, \eta) \xi_{T_i T_f}^{(l\eta)}(\mathcal{E}_x, \mathcal{E}_y). \quad (6.1)$$

Here, $M_{fi}(l, \eta)$ is the product of two interaction matrix elements appropriate to the process, c_η is 1 if the intermediate state is a photon and $-\eta$ if it is a fermion, and

$$\begin{aligned} \xi_{T_i T_f}^{(l\eta)}(\mathcal{E}_x, \mathcal{E}_y) &\equiv e^{+(\gamma_{i1} + \gamma_{i2})T_i/2 - (\gamma_{f1} + \gamma_{f2})T_f/2} e^{+i(e_{i1} + e_{i2})T_i - i(e_{f1} + e_{f2})T_f} \\ &\times \int_{T_i}^{T_f} dx^0 \int_{T_i}^{T_f} dy^0 \theta[\eta(x^0 - y^0)] \exp[-i\eta\mathcal{E}_l(x^0 - y^0) - i\mathcal{E}_x x^0 - i\mathcal{E}_y y^0]. \quad (6.2) \end{aligned}$$

The factor $e^{+(\gamma_{i1}+\gamma_{i2})T_i/2-(\gamma_{f1}+\gamma_{f2})T_f/2}$ in Eq. (6.2) adjusts the normalization of the initial and final states to be 1 at T_i and T_f , respectively, while the factor $e^{+i(e_{i1}+e_{i2})T_i-i(e_{f1}+e_{f2})T_f}$ allows a convenient choice of phase. The quantity $\xi_{T_i T_f}^{(l\eta)}(\mathcal{E}_x, \mathcal{E}_y)$ is the new object which incorporates the resonant energy denominators and in general replaces the energy-conserving δ -function. It may be calculated by the substitution $u = x^0 - y^0$, $v = x^0 + y^0$. The result is

$$\begin{aligned} \xi_{T_i T_f}^{(l\eta)}(\mathcal{E}_x, \mathcal{E}_y) = & \frac{e^{+(\gamma_{i1}+\gamma_{i2})T_i/2-(\gamma_{f1}+\gamma_{f2})T_f/2} e^{+i(e_{i1}+e_{i2})T_i-i(e_{f1}+e_{f2})T_f}}{\mathcal{E}_x + \mathcal{E}_y} \\ & \times \left\{ \frac{e^{-i(\mathcal{E}_x+\mathcal{E}_y)T_f} [e^{(i/2)[(1-\eta)\mathcal{E}_x+(1+\eta)\mathcal{E}_y-2\mathcal{E}_l}(T_f-T_i) - 1]}{(1/2)[(1-\eta)\mathcal{E}_x + (1+\eta)\mathcal{E}_y - 2\mathcal{E}_l]} \right. \\ & \left. - \frac{e^{-i(\mathcal{E}_x+\mathcal{E}_y)T_i} [e^{(i/2)[(-1-\eta)\mathcal{E}_x+(-1+\eta)\mathcal{E}_y-2\mathcal{E}_l}(T_f-T_i) - 1]}{(1/2)[(-1-\eta)\mathcal{E}_x + (-1+\eta)\mathcal{E}_y - 2\mathcal{E}_l]} \right\}. \end{aligned} \quad (6.3)$$

Eq. (6.3) provides an expression which may be adapted to any second-order process of interest by adjusting the μ and the assignments of the e and γ to the E and Γ . In the particular case of two-particle to two-particle scattering we need consider four cases: the ‘‘direct’’ and ‘‘cross’’ diagrams (Fig. 4), each for $\eta = \pm 1$. The expressions are simplified by the notation $\Delta e \equiv e_{i1} + e_{i2} - e_{f1} - e_{f2}$, $\Delta\gamma \equiv \gamma_{i1} + \gamma_{i2} - \gamma_{f1} - \gamma_{f2}$, and $\tau \equiv T_f - T_i$.

a. Direct diagram, $\eta = +1$ We obtain this case from Eq. (6.3) by setting $\mathcal{E}_x = -(e_{f1} + e_{f2}) + i(\gamma_{f1} + \gamma_{f2})/2$ and $\mathcal{E}_y = (e_{i1} + e_{i2}) - i(\gamma_{i1} + \gamma_{i2})/2$. We obtain

$$\begin{aligned} \xi_{T_i T_f}^{(l,+1)}(\mathcal{E}_x, \mathcal{E}_y) = & \frac{1}{\Delta e - i\Delta\gamma/2} \times \left\{ \frac{e^{-i(E_l - i\Gamma_l/2)\tau} - e^{-i[(e_{i1}+e_{i2})-i(\gamma_{i1}+\gamma_{i2})/2]\tau}}{(e_{i1} + e_{i2} - E_l) - i(\gamma_{i1} + \gamma_{i2} - \Gamma_l)/2} \right. \\ & \left. - \frac{e^{-i(E_l - i\Gamma_l/2)\tau} - e^{-i[(e_{f1}+e_{f2})-i(\gamma_{f1}+\gamma_{f2})/2]\tau}}{(e_{f1} + e_{f2} - E_l) - i(\gamma_{f1} + \gamma_{f2} - \Gamma_l)/2} \right\}. \end{aligned} \quad (6.4)$$

b. Direct diagram, $\eta = -1$ For the same assignments as case (a), but with $\eta = -1$, we find

$$\begin{aligned} \xi_{T_i T_f}^{(l,-1)}(\mathcal{E}_x, \mathcal{E}_y) = & \frac{1}{\Delta e - i\Delta\gamma/2} \\ & \times \left\{ \frac{e^{-i[(e_{i1}+e_{i2}+e_{f1}+e_{f2}+E_l)-i(\gamma_{i1}+\gamma_{i2}+\gamma_{f1}+\gamma_{f2}+\Gamma_l)/2]\tau} - e^{-i[(e_{i1}+e_{i2})-i(\gamma_{i1}+\gamma_{i2})/2]\tau}}{(-e_{f1} - e_{f2} - E_l) - i(-\gamma_{f1} - \gamma_{f2} - \Gamma_l)/2} \right. \\ & \left. - \frac{e^{-i[(e_{i1}+e_{i2}+e_{f1}+e_{f2}+E_l)-i(\gamma_{i1}+\gamma_{i2}+\gamma_{f1}+\gamma_{f2}+\Gamma_l)/2]\tau} - e^{-i[(e_{f1}+e_{f2})-i(\gamma_{f1}+\gamma_{f2})/2]\tau}}{(-e_{i1} - e_{i2} - E_l) - i(-\gamma_{i1} - \gamma_{i2} - \Gamma_l)/2} \right\}. \end{aligned} \quad (6.5)$$

c. Cross diagram, $\eta = +1$ Here we set $\mathcal{E}_x = (e_{i2} - e_{f2}) - i(\gamma_{i2} - \gamma_{f2})/2$ and $\mathcal{E}_y = (e_{i1} - e_{f1}) - i(\gamma_{i1} - \gamma_{f1})/2$:

$$\begin{aligned} \xi_{T_i T_f}^{(l,+1)}(\mathcal{E}_x, \mathcal{E}_y) = & \frac{1}{\Delta e - i\Delta\gamma/2} \times \left\{ \frac{e^{-i[(e_{f1}+e_{i2}+E_l)-i(\gamma_{f1}+\gamma_{i2}+\Gamma_l)/2]\tau} - e^{-i[(e_{i1}+e_{i2})-i(\gamma_{i1}+\gamma_{i2})/2]\tau}}{(e_{i1} - e_{f1} - E_l) - i(\gamma_{i1} - \gamma_{f1} - \Gamma_l)/2} \right. \\ & \left. - \frac{e^{-i[(e_{f1}+e_{i2}+E_l)-i(\gamma_{f1}+\gamma_{i2}+\Gamma_l)/2]\tau} - e^{-i[(e_{f1}+e_{f2})-i(\gamma_{f1}+\gamma_{f2})/2]\tau}}{(e_{f2} - e_{i2} - E_l) - i(\gamma_{f2} - \gamma_{i2} - \Gamma_l)/2} \right\}. \end{aligned} \quad (6.6)$$

d. *Cross diagram*, $\eta = -1$ The assignments here are as in case (c), and $\eta = -1$:

$$\xi_{T_i T_f}^{(l,-1)}(\mathcal{E}_x, \mathcal{E}_y) = \frac{1}{\Delta e - i\Delta\gamma/2} \times \left\{ \frac{e^{-i[(e_{f2}+e_{i1}+E_l)-i(\gamma_{f2}+\gamma_{i1}+\Gamma_l)/2]\tau} - e^{-i[(e_{i1}+e_{i2})-i(\gamma_{i1}+\gamma_{i2})/2]\tau}}{(e_{i2} - e_{f2} - E_l) - i(\gamma_{i2} - \gamma_{f2} - \Gamma_l)/2} - \frac{e^{-i[(e_{f2}+e_{i1}+E_l)-i(\gamma_{f2}+\gamma_{i1}+\Gamma_l)/2]\tau} - e^{-i[(e_{f1}+e_{f2}+E_l)-i(\gamma_{f1}+\gamma_{f2}+\Gamma_l)/2]\tau}}{(e_{f1} - e_{i1} - E_l) - i(\gamma_{f1} - \gamma_{i1} - \Gamma_l)/2} \right\}. \quad (6.7)$$

The expressions in Eqs. (6.4), (6.5), (6.6), and (6.7) all contain products of two complex energy denominators, one “energy-conserving” and the other resonant. All these energy denominators may in principle go to zero. When this happens, however, there is always a cancellation of the exponentials in the numerators, so that the result is always finite. This is a consequence of the fact that these expressions were derived starting from Eq. (6.2), an integral over a finite range of a finite integrand, which consequently may never diverge. Therefore, scattering processes containing virtual fermions now have finite S-matrix elements. These were the last remaining resonant divergences in the theory, *which is now entirely finite*.

We have thus eliminated all resonant divergences from our scattering cross-sections. The price we have paid is the dependence of the S-matrix elements on the time lapse τ between the preparation of the initial state and the measurement of the final state, and the attendant loss of strict energy conservation. Note that in general, the nature of the dependence on τ is for the S-matrix elements to decay away as $\tau \rightarrow \infty$. As discussed in the previous section, this is the behavior expected for scattering from excited states to excited states.

Note also that these expressions lack crossing symmetry. The reason is the introduction of the exponential factor outside the integral in Eq. (6.3), which is not symmetric under the replacement $e_{i1} \leftrightarrow -e_{f2}$, $\gamma_{i1} \leftrightarrow -\gamma_{f2}$. If we divide the expressions of Eqs. (6.4), (6.5), (6.6), and (6.7) by the exponential factor we find that the resulting expressions are, in fact, crossing symmetric.

In order to parlay the above expressions into cross-sections, we must substitute them into Eq. (6.1) to obtain a τ -dependent expression for the S-matrix element. The reaction rate R is then given by $R = d|S_{fi}|^2/d\tau = 2\text{Re}\{S_{fi}^* dS_{fi}/d\tau\}$. The cross-section may be obtained from R by the usual kinematic manipulation: $d\sigma/d\Omega_f = L^3|\mathbf{v}|^{-1}R$, where $d\Omega_f$ is a volume element in the space of final states and \mathbf{v} is the relative velocity of the initial particles.

There are two special cases where it is possible to eliminate the dependence on τ from these expressions: when the initial state is stable ($\gamma_{i1} = \gamma_{i2} = 0$), and when the final state is stable ($\gamma_{f1} = \gamma_{f2} = 0$). These cases are called “absorption” and “emission” scattering, respectively. In the absorption scattering case, we may set $T_i \rightarrow -\infty$, while in the emission scattering case we may set $T_f \rightarrow \infty$. In either case, $\tau \rightarrow \infty$, and the above expressions for the ξ are greatly simplified.

A. Absorption scattering

The special case of a stable initial state corresponds to a situation analogous to absorption, in which we prepare beams of stable particles and observe the excited products before they have the opportunity to decay. If we set $\gamma_{i1} = \gamma_{i2} = 0$ in Eqs. (6.4), (6.5), (6.6), and (6.7), and take the limit $\tau \rightarrow \infty$, we find the following results:

For the direct diagram,

$$\xi_{-\infty, T_f}^{(l,+1)}(\mathcal{E}_x, \mathcal{E}_y) = \frac{1}{(\Delta e - i\Delta\gamma/2)[(-e_{i1} - e_{i2} + E_l) - i\Gamma_l/2]}, \quad (6.8a)$$

$$\xi_{-\infty, T_f}^{(l,-1)}(\mathcal{E}_x, \mathcal{E}_y) = \frac{1}{(\Delta e - i\Delta\gamma/2)[(e_{f1} + e_{f2} + E_l) - i(\gamma_{f1} + \gamma_{f2} + \Gamma_l)/2]}, \quad (6.8b)$$

and for the cross diagram,

$$\xi_{-\infty, T_f}^{(l,+1)}(\mathcal{E}_x, \mathcal{E}_y) = \frac{1}{(\Delta e - i\Delta\gamma/2)[(e_{f1} - e_{i1} + E_l) - i(\gamma_{f1} + \Gamma_l)/2]}, \quad (6.9a)$$

$$\xi_{-\infty, T_f}^{(l,-1)}(\mathcal{E}_x, \mathcal{E}_y) = \frac{1}{(\Delta e - i\Delta\gamma/2)[(e_{f2} - e_{i2} + E_l) - i(\gamma_{f2} + \Gamma_l)/2]}. \quad (6.9b)$$

We have eliminated an inessential phase factor. Note that $\Delta\gamma = -(\gamma_{f1} + \gamma_{f2})$. Substituting these expressions in Eq. (6.1), we obtain a time-independent S-matrix element. In order to get the result into the form of a cross-section, note that the final state is decaying at a rate $\gamma_{f1} + \gamma_{f2}$. In order that the probability of that final state be time-independent and equal to $|S_{fi}|^2$, the reaction rate must exactly balance the decay rate, so that we must have $R = (\gamma_{f1} + \gamma_{f2})|S_{fi}|^2 = |\Delta\gamma||S_{fi}|^2$. Again, cross-section $d\sigma/d\Omega_f$ may be trivially obtained from R . Note that $d\sigma/d\Omega_f$ contains the following functional dependence on Δe :

$$\frac{d\sigma}{d\Omega_f} \propto \frac{|\Delta\gamma|}{\Delta e^2 + (\Delta\gamma/2)^2} \xrightarrow{\Delta\gamma \rightarrow 0} 2\pi \delta(e_{i1} + e_{i2} - e_{f1} - e_{f2}). \quad (6.10)$$

In other words, the energy conservation in the cross-section is Lorentzian, and in the limit of stable final states we recover the energy-conserving δ -function with the correct coefficient of 2π . As expected, the strict energy conservation in the old expressions for the S-matrix elements is correct for scattering from stable states to stable states.

B. Emission scattering

The special case of a stable final state corresponds to a situation analogous to emission, in which we prepare a beam of excited particles and observe them after they have scattered into the stable final state. We set $\gamma_{f1} = \gamma_{f2} = 0$ in Eqs. (6.4), (6.5), (6.6), and (6.7), and take the limit $\tau \rightarrow \infty$, to obtain:

For the direct diagram,

$$\xi_{T_i, \infty}^{(l,+1)}(\mathcal{E}_x, \mathcal{E}_y) = \frac{1}{(\Delta e - i\Delta\gamma/2)[(e_{f1} + e_{f2} + E_l) - i\Gamma_l/2]}, \quad (6.11a)$$

$$\xi_{T_i, \infty}^{(l,-1)}(\mathcal{E}_x, \mathcal{E}_y) = \frac{1}{(\Delta e - i\Delta\gamma/2)[(e_{i1} + e_{i2} + E_l) - i(\gamma_{i1} + \gamma_{i2} + \Gamma_l)/2]}, \quad (6.11b)$$

and for the cross diagram,

$$\xi_{T_i, \infty}^{(l, +1)}(\mathcal{E}_x, \mathcal{E}_y) = \frac{1}{(\Delta e - i\Delta\gamma/2)[(e_{i2} - e_{f2} + E_l) - i(\gamma_{i2} + \Gamma_l)/2]}, \quad (6.12a)$$

$$\xi_{T_i, \infty}^{(l, -1)}(\mathcal{E}_x, \mathcal{E}_y) = \frac{1}{(\Delta e - i\Delta\gamma/2)[(e_{i1} - e_{f1} + E_l) - i(\gamma_{i1} + \Gamma_l)/2]}. \quad (6.12b)$$

Once again, we have eliminated an inessential phase from the amplitudes. Now we have $\Delta\gamma = \gamma_{i1} + \gamma_{i2}$. Substituting these expressions in Eq. (6.1), we again obtain a time-independent S-matrix element. We obtain a cross-section by the argument illustrated in Fig. 5, which depicts a semi-infinite tube of cross-sectional area $d\sigma/d\Omega_f$, terminating at the position of the target particle and extending in the direction of $-\mathbf{v}$. The total probability (per unit final phase-space volume) of an interaction leading to a final state in $d\Omega_f$ is equal to the integral over the interior of the tube of the probability that each infinitesimal slice should contain the projectile particle *and* that it should actually reach the target particle in spite of the fact that the two-particle state is decaying away:

$$|S_{fi}|^2 = L^{-3} \int_0^\infty |\mathbf{v}| dt \frac{d\sigma}{d\Omega_f} e^{-(\gamma_{i1} + \gamma_{i2})t} = \frac{|\mathbf{v}|}{\Delta\gamma L^3} \frac{d\sigma}{d\Omega_f}, \quad (6.13)$$

so that

$$\frac{d\sigma}{d\Omega_f} = L^3 |\mathbf{v}|^{-1} \Delta\gamma |S_{fi}|^2. \quad (6.14)$$

We again see the Lorentzian energy conservation of Eq. (6.10), so that in this case we also recover strict energy conservation for stable state to stable state scattering.

VII. DISCUSSION

The regime of validity of the “emission” and “absorption” scattering limits is obvious from their context. On the other hand, the general formula in Eq. (6.3) requires some discussion. As discussed previously, the formula never “misbehaves”, in the sense that it never yields a divergent result. In fact, in general that result tends to zero as $\tau \rightarrow \infty$. While this is physically sensible, it obviously makes the large time-lapse limit a less than useful one. It is clear that what fails in this limit is the validity of the perturbation-theoretic order of the calculation. Since the scattering states are themselves decaying to other states, those other states should be included in the calculation, leading to higher-order processes. The second-order calculations outlined in the previous section are only useful for values of τ such that the scattering states have little chance to decay, that is for $\Gamma\tau \ll 1$, where Γ is the largest of the decay rates in the process. For example, we might choose τ to be on the order of a collision time, if we are studying a gas with density and temperature such that the collision rates far exceed the decay rates.

The general case above obviously represents a fairly radical departure from the usual scattering formulae. The “emission” and “absorption” scattering limits amount to somewhat less

radical modifications. One obvious such modification is the replacement of strict energy conservation with “Lorentzian” energy conservation. Another is that the “non-resonant” energy denominators [Eqs. (6.8b), (6.9a), (6.9b), (6.11b), (6.12a), (6.12b)] now contain the decay rates of the scattering states as well as those of the intermediate states. The importance of these changes depends upon whether the decay widths entering the energy denominators are electron decay widths or photon decay widths.

If the decay widths are purely fermionic, they are gently varying functions of energy, and their magnitudes are smaller by e^2 than their own characteristic scale of variation, the scale of variation of the interaction matrix elements, and the characteristic separation of the resonances. Consequently, in this case the relative change that results from introducing Lorentzian, rather than exact, energy conservation, and from introducing the decay widths of the scattering states into the energy denominators, is of order e^2 . On the other hand, if some of the decay widths correspond to photon lines, they can vary rather rapidly as a function of energy [11,12]. Thus, the behavior of the energy denominators is not really “Lorentzian”, despite notational appearances to the contrary. The departure from the cross-sections computed assuming strict energy conservation and not including external line decay widths might turn out to be appreciable in this case, although its precise magnitude remains to be assessed.

In the limit of stable scattering states the usual results are completely reproduced, since we recover strict energy conservation and there are no scattering state decay widths to include in resonant energy denominators.

In connection with the dressed photon propagator of Eq. (4.11), we wish to comment on a point which is a potential source of confusion. The decay width $\Gamma(\mathbf{k}, j)$ is to be evaluated on the light cone, as implied by the first line of Eq. (4.10). Now, when the photon propagator is used in an S-matrix element, the values of k^0 , k^2 , and k^3 are fixed by the x^0 , x^2 , and x^3 momenta of the scattering states. Thus, the sum over intermediate photon wave states involves an integral over the component k^1 of the wave vector \mathbf{k} . The value of $\Gamma(\mathbf{k}, j)$ must be evaluated for *each* value of k^1 in the integral. This is analogous to the case of the electron propagator, Eq. (3.4), in which the intermediate electron decay width is evaluated, on the energy shell, for each Landau level in the sum over intermediate states. The only difference between the two cases is that the relevant degrees of freedom are discrete for the electron propagator, while they are continuous for the photon propagator.

The radiatively corrected photon propagator permits for the first time the evaluation of processes such as $e^+e^- \rightarrow e^+e^-$, $e^- \rightarrow e^-e^+e^-$, and $\gamma e^- \rightarrow e^-e^+e^-$, all of which are important for neutron star emission. Of equal astrophysical importance is the evaluation above the one photon pair-production threshold of Compton scattering, two photon pair annihilation, and two photon pair production, which is now possible by virtue of the radiatively corrected scattering states. Finally, we now have access to the processes $e^-e^- \rightarrow e^-e^-$ and $e^+e^- \rightarrow e^+e^-$ even when the initial and final states are excited.

VIII. ACKNOWLEDGMENTS

While this work was performed, Carlo Graziani held a National Research Council-NASA Goddard Space Flight Center Research Associateship.

REFERENCES

- [1] J. Trumper *et al.*, *Astrophys. J.* **219**, L105 (1978).
- [2] D. E. Gruber *et al.*, *Astrophys. J.* **240**, L127 (1980).
- [3] A. K. Harding, *Science* **251**, 1033 (1991).
- [4] J. H. Taylor and D. R. Stinebring, *Annu. Rev. Astron. Astrophys.* **24**, 285 (1986).
- [5] T. Murakami *et al.*, *Nature* **335**, 234 (1988).
- [6] R. C. Duncan and C. Thompson, *Astrophys. J.* **392**, L9 (1992).
- [7] B. Paczyński, *Acta Astron.* **42**, 145 (1992).
- [8] J. K. Daugherty and J. Ventura, *Phys. Rev. D* **18**, 4 (1978).
- [9] D. B. Melrose and V. V. Zheleznyakov, *Astron. Astrophys.* **95**, 86 (1981).
- [10] H. Herold, H. Ruder, and G. Wunner, *Astron. Astrophys.* **115**, 90 (1982).
- [11] N. P. Klepikov, *Zh. Eksp. Teor. Fiz.*, **26**, 19 (1954).
- [12] J. K. Daugherty and A. K. Harding, *Astrophys. J.* **273**, 761 (1983).
- [13] G. Wunner, *Phys. Rev. Lett.* **42**, 79 (1979).
- [14] J. K. Daugherty and R. W. Bussard, *Astrophys. J.* **238**, 296 (1980).
- [15] A. K. Harding, *Astrophys. J.* **300**, 167 (1986).
- [16] G. Wunner, J. Paez, H. Herold, and H. Ruder, *Astron. Astrophys.* **170**, 179 (1986).
- [17] H. Herold, *Phys. Rev. D*, **19**, 2868 (1979).
- [18] J. K. Daugherty and A. K. Harding, *Astrophys. J.* **309**, 362 (1986).
- [19] R. W. Bussard, S. B. Alexander, and P. Mészáros, *Phys. Rev. D* **34**, 440 (1986).
- [20] A. K. Harding and J. K. Daugherty, *Astrophys. J.* **374**, 687 (1991).
- [21] A. A. Kozlenkov and I. G. Mitrofanov, *Sov. Phys. JETP*, **64**, 1173 (1986).
- [22] S. H. Langer, *Phys. Rev. D*, **23**, 328 (1981).
- [23] C. Graziani, *Astrophys. J.* **412**, 351 (1993).
- [24] J. D. Bjorken, and S. D. Drell, *Relativistic Quantum Mechanics*, (McGraw-Hill, New York, 1964), p. 95.
- [25] M. H. Johnson and B. A. Lippmann, *Phys. Rev.* **76**, 828 (1949).
- [26] D. B. Melrose and A. J. Parle, *Aust. J. Phys.*, **36**, 755 (1983).
- [27] A. J. Parle, *Aust. J. Phys.*, **40**, 1 (1987).
- [28] A. A. Sokolov and I. M. Ternov, *Synchrotron Radiation* (Akademie, Berlin, 1968).
- [29] I. A. Batalin and A. E. Shabad, *Sov. Phys. JETP*, **33**, 483 (1971).
- [30] A. E. Shabad, *Ann. Phys. (NY)*, **90**, 166 (1975).
- [31] D. B. Melrose and R. J. Stoneham, *Nuovo Cimento A*, **32**, 435 (1976).
- [32] N. N. Bogoliubov and D. V. Shirkov, *Introduction to the Theory of Quantized Fields* (Interscience, London, 1959), Sec. 31.5.
- [33] J. S. Toll, Ph.D. Thesis, Princeton University, 1952.

FIGURES

FIG. 1. Two diagrams for e^+e^- scattering. The labels a_i^+ , a_i^- denote the x^1 -coordinate of the orbit center of the initial positron and electron, respectively, while the labels a_f^+ , a_f^- denote the orbit center of the final positron and electron, respectively. The spatial separation between the two fermion lines is given by the parameter $s = a_f^+ - a_f^-$ for (a), and by $t = a_f^- - a_i^-$ for (b). In either case the interaction does not fall off with increasing separation, so that the result is a divergence in the total cross-section.

FIG. 2. Processes allowing non-decaying, on-shell virtual states; (a) $e^-\gamma$ scattering; (b) e^-e^- scattering. The process in (a) may be viewed as a pair production followed by a pair annihilation. When the intermediate positron is in the Landau ground state it has zero decay width. Similarly, the process in (b) may be viewed as cyclotron emission followed by cyclotron absorption. The decay width of the intermediate state vanishes if it is below the one photon pair-production threshold.

FIG. 3. Generic scattering diagram. The lines may be either fermion or photon lines, and the external lines may be either incoming ($\mu = +1$) or outgoing ($\mu = -1$).

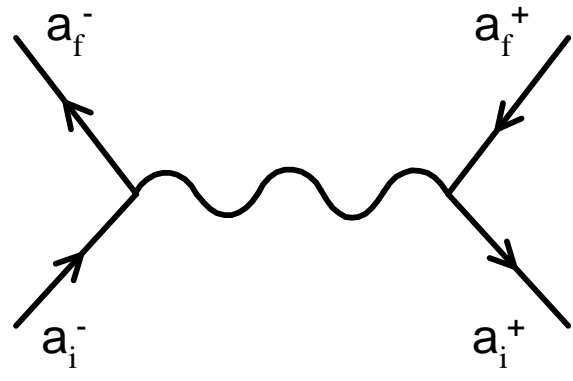
FIG. 4. Generic “direct” and “cross” diagrams. The lines may be either fermion or photon lines.

FIG. 5. Kinematics of emission scattering. The target particle is at the end face of the semi-infinite tube of cross-sectional area $d\sigma/d\Omega_f$. The projectile particle must be in the tube in order for an interaction to occur. The decreasing density of circular sections in the figure is meant to represent the decreasing probability of an interaction due to the exponential decay of the initial state.

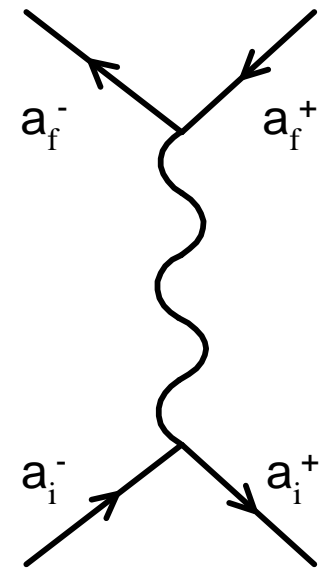
This figure "fig1-1.png" is available in "png" format from:

<http://arxiv.org/ps/astro-ph/9503086v1>

t
↑



(a)



(b)

Figure 1

This figure "fig1-2.png" is available in "png" format from:

<http://arxiv.org/ps/astro-ph/9503086v1>

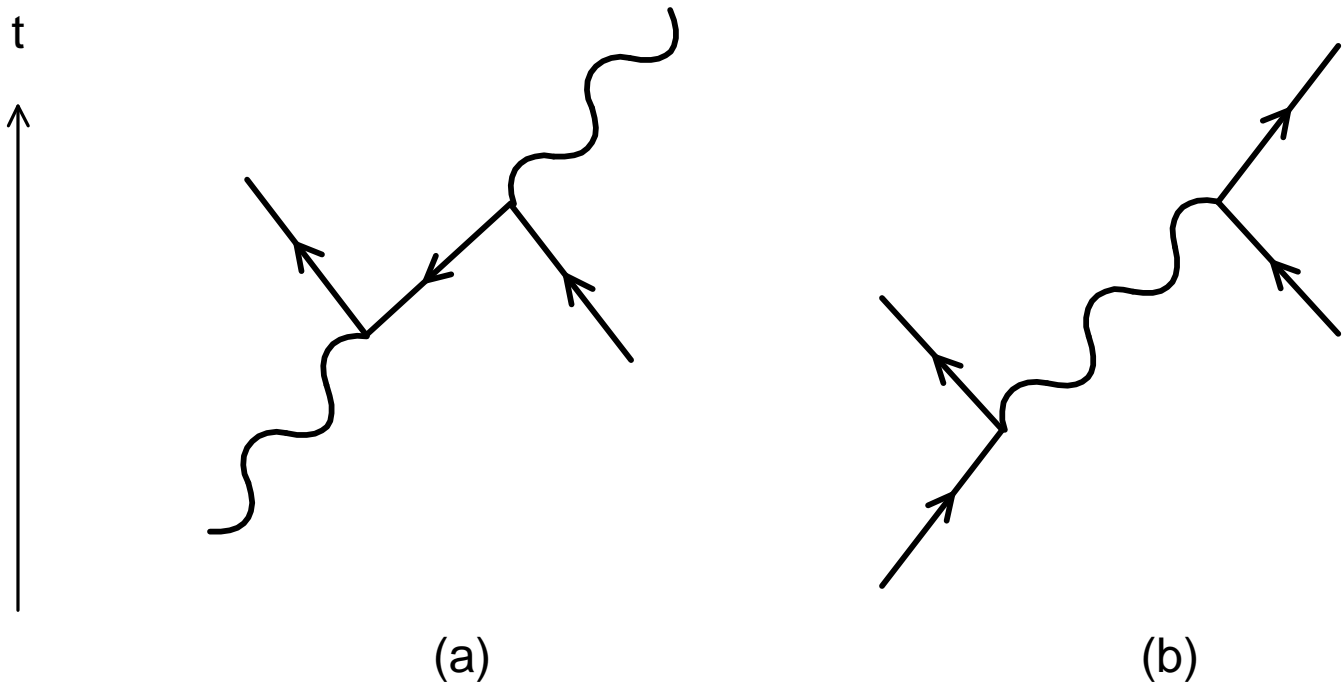


Figure 2

This figure "fig1-3.png" is available in "png" format from:

<http://arxiv.org/ps/astro-ph/9503086v1>

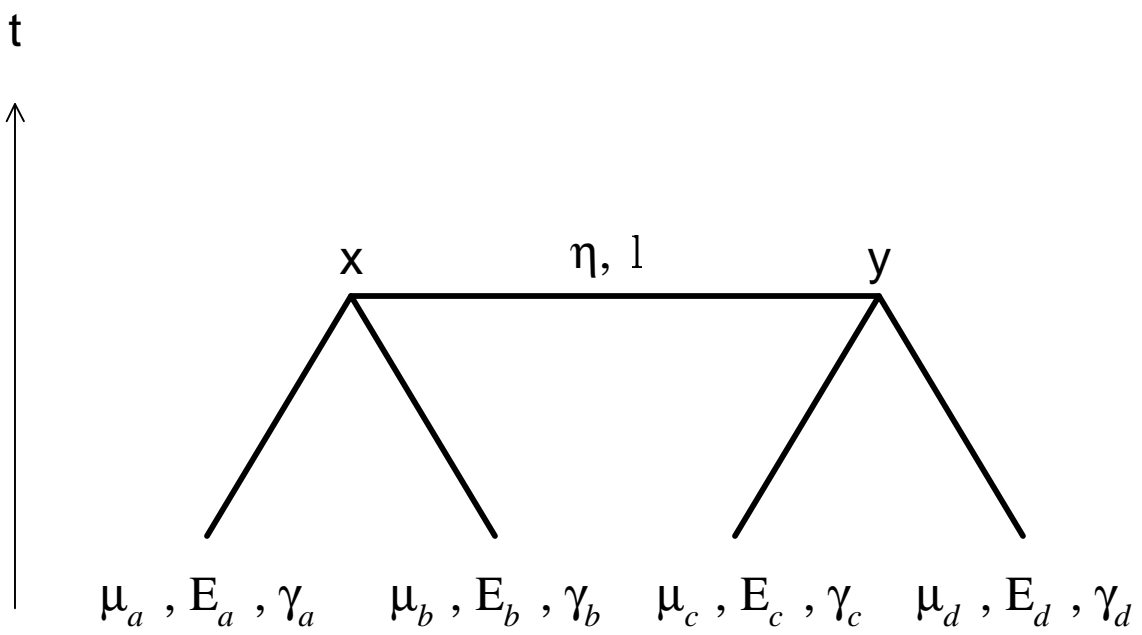


Figure 3

This figure "fig1-4.png" is available in "png" format from:

<http://arxiv.org/ps/astro-ph/9503086v1>

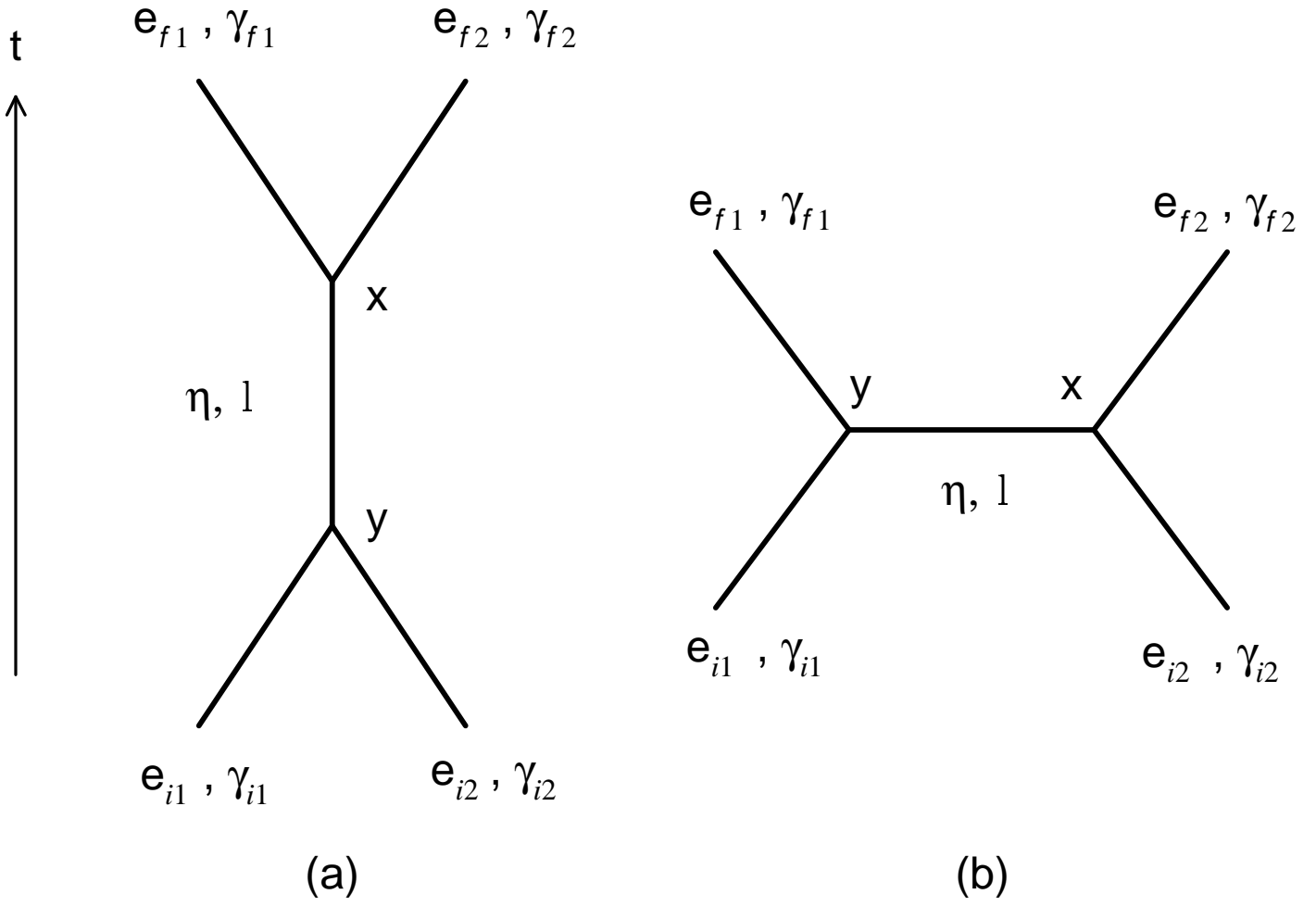


Figure 4

This figure "fig1-5.png" is available in "png" format from:

<http://arxiv.org/ps/astro-ph/9503086v1>

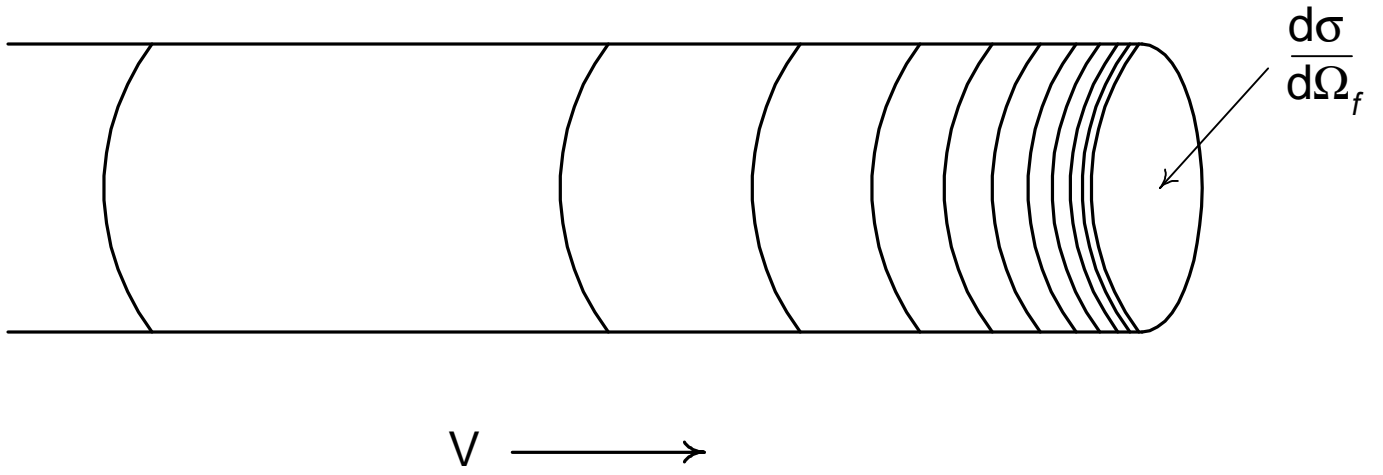


Figure 5